Organic Field Effect Transistors Based on Biphenyl, Fluorene End-Capped Fused Bithiophene Oligomers

Yong-Young Noh,[†] Reiko Azumi,[‡] Midori Goto,[§] Byung-Jun Jung,[||] Eunhee Lim,[||] Hong-Ku Shim,*[,||] Yuji Yoshida,[⊥] Kiyoshi Yase,*[,⊥] and Dong-Yu Kim*[,†]

Center for Frontier Materials, Department of Materials Science and Engineering, Gwangju Institute of Science and Technology (GIST), 1 Oryong-Dong, Buk-Gu, Gwangju 500-712, South Korea, Center for Advanced Functional Polymers, Department of Chemistry and School of Molecular Science (BK21), Korea Advanced Institute of Science and Technology (KAIST), Daejeon 305-701, South Korea, Nanotechnology Research Institute and Research Facilities Department, Technical Service Center, National Institute of Advanced Industrial Science and Technology (AIST), Tsukuba Central 5-2, Higashi 1-1-1, Tsukuba 305-8565, Japan, and Photonics Research Institute, National Institute of Advanced Industrial Science and Technology (AIST), 1-1-1 Higashi, Tsukuba, Ibaraki 305-8565, Japan

Received March 4, 2005. Revised Manuscript Received May 22, 2005

Organic field effect transistors based on a structural combination of fused bithiophene with fluorene (BFTT) or biphenyl units (BPTT) are described. The two molecules have similar molecular structures, except that the fluorene unit of BFTT is substituted for a biphenyl in BPTT. A 1.5−2 times higher field effect mobility was achieved with BPTT compared to that of BFTT. To determine the reason for the superior mobility of BPTT compared to that of BFTT, single-crystal X-ray structures of BPTT and BFTT were determined and a clear correlation between the crystal structure and the electrical characteristics was found. The BFTT based on a fluorene unit adopts a slightly more distorted conformation that deviates from the quasi-planar structure in the single crystal with larger dihedral and bending angles than those of BPTT. On the other hand, BPTT shows a quite planar structure with relatively small dihedral and bending angles. BFTT also shows longer shortest intermolecular distances than BPTT. Those are the results of the carbon at the 9 position of fluorene units and attached hydrogen atoms on that position in BFTT, which is regarded as the only difference of the two molecules. These differences in molecular conformation and packing characteristics in the single-crystal consequently affect the transport properties of the electric carrier. In addition, device stability was checked after storage in air for more than 1 month or after exposure to strong UV irradiation for several hours. Both molecules showed a high device stability, but BPTT was slightly better. This better air and UV stability of biphenyl-based BPTT, compared to fluorene-based BFTT, can be attributed to the lower highest occupied molecular orbital energy level of the BPTT and keto-defect formation in the fluorene unit of BFTT, after UV irradiation.

Introduction

Conjugated organic semiconductors have been a subject of considerable interest, not only for the exploration of their fundamental structure−property relationships, specifically, for their electrical or optical properties, but also for applications to various organic-based devices such as organic field effect transistors (OFETs), organic light emitting diodes (OLEDs), and photovoltaic cells (PVs).[1] In particular, these materials can show a high mobility of charge carriers, when the molecules are closely packed in thin films in a controlled manner or packed as a single crystal.[2] The field effect mobility (μ_{FET}), one of the key parameters in OFETs, is strongly dependent on the distance between molecules, which can be controlled by intermolecular secondary interactions, and on the packing, such as herringbone or π stacking.[3] Therefore, a study of the effects of conformation and molecular packing properties in a single crystal of conjugated oligomers or the orientation of molecules, as this relates to electrical properties, that is, the charge carrier mobility, is one of the most important and interesting research topics for fundamental studies of semiconducting materials with a

* To whom correspondence should be addressed. E-mail: kimdy@gist.ac.kr (D.-Y.K); hkshim@kaist.ac.kr (H.-K.S); k.yase@aist.go.jp (K.Y).
[†] Gwangju Institute of Science and Technology (GIST).
[‡] Nanotechnology Research Institute, National Institute of Advanced Industrial Science and Technology (AIST).
[§] Technical Service Center, National Institute of Advanced Industrial Science and Technology (AIST).
[||] Korea Advanced Institute of Science and Technology (KAIST).
[⊥] Photonics Research Institute, National Institute of Advanced Industrial Science and Technology (AIST).

(1) (a) Horowitz, G. *Adv. Mater*. **1998**, *10*, 365. (b) Katz, H. E.; Bao, Z. *J. Phys. Chem. B* **2000**, *104*, 671. (c) Dimitrakopoulos, C. D.; Malenfant, P. R. L. *Adv. Mater*. **2002**, *14*, 99. (d) Friend, R. H.; Gymer, R. W.; Holmes, A. B.; Burroughes, J. H.; Marks, R. N.; Taliani, C.; Bradley, D. D. C.; Dossantos, D. A.; Bredas, J. L.; Lögdlund, M.; Salaneck, W. R. *Nature* **1999**, *397*, 121. (e) Peumans, P.; Yakimov, A.; Forrest, S. R. *J. Appl. Phys.* **2003**, *93*, 3693. (f) Brabec, C. J.; Sariciftci, N. S.; Hummelen, J. C. *Adv. Funct. Mater.* **2001**, *11*, 15.

(2) (a) Dimitrakopoulos, C. D.; Brown, A. R.; Pomp, A. *J. Appl. Phys*. **1996**, *80*, 2501. (b) Sirringhaus, H.; Brown, P. J.; Friend, R. H.; Nielsen, M. M.; Bechgaard, K.; Langeveld-Voss, B. M. W.; Spiering, A. J. H.; Janssen, R. A. J.; Meijer, E. W.; Herwig, P.; De Leeuw, D. M. *Nature* **1999**, *401*, 685. (c) Noh, Y.-Y.; Kim, J.-J.; Yoshida, Y.; Yase, K. *Adv. Mater*. **2003**, *15*, 699. (d) Nagamatsu, S.; Tanigaki, N.; Yoshida, Y.; Takashima, W.; Yase, K.; Kaneto, K. *Synth. Met.* **2003**, *137*, 923. (e) van de Craats, A. M.; Stutzmann, N.; Bunk, O.; Nielsen, M. M.; Watson, M.; Müllen, K.; Chanzy, H. D.; Sirringhaus, H.; Friend, R. H. *Adv. Mater*. **2003**, *15*, 495. (f) Yanagi, H.; Araki, Y.; Ohara, T.; Hotta, S.; Ichikawa, M.; Taniguchi, Y. *Adv. Funct. Mater*. **2003**, *13*, 767.

10.1021/cm0504889 CCC: $30.25
Published on Web 06/18/2005

high mobility for OFETs.[4] Moreover, the electrical properties of polymers, which are relatively difficult to predict compared to those of small molecules, could be more easily understood by means of studies on their oligomeric analogues.[5]

Oligophenylenes and oligothiophenes have attracted considerable attention, due to their good performance for p-type semiconductors.[6] Thiophene oligomers, in particular, have been considered to be one of the promising building blocks with various modification possibilities because they show a variety of intra- and intermolecular interactions, which are related to the plasticity of the thiophene ring, which has a large polarity.[7] During the past decade, a number of research groups have reported extensive results related to the effect of structure and/or packing properties of single crystals of oligothiophene derivatives on their electrical properties.[3,8] Unfortunately, most p-channel oligothiophenes are easily oxidized, due to the relatively low band gap and high highest occupied molecular orbital (HOMO) levels.[9] Therefore, they showed poor device stability, most notably a temporal decrease in the current ratio of the on−off ratio (I_{ON}/I_{OFF}), which resulted from a large increase in the off current by unintended oxygen doping, thus, making them unsuitable for practical electronic circuit applications without careful encapsulation. To overcome this problem, organic subunits such as thiazolidene or phenylene have been introduced in oligothiophene via co-oligomerization, in an attempt to modulate HOMO levels.[10] Another approach for obtaining a low HOMO level is to prepare a fused structure from an unfused molecule with the same component of building blocks. The fused molecule could have a relatively lower HOMO level than an unfused one via a widening in the electrical band gap which results from a shorter effective conjugation length.[3e] An oligofluorene end-capped thiophene, 5,5′-bis(9*H*-fluorene-2-yl)-[2,2′]bithiophene (FTTF), was also recently introduced as a high performance p-type active material, which had better air and UV stability.[11] Such fluorene moieties have widely been used as building blocks for OLEDs, PVs, organic lasers, sensors, and OFETs due to their high thermal stability, fluorescence quantum yield, and mesogenic properties resulting from their rigid structures with less conformational freedom.[12] Even though such materials have been extensively studied because of their high performance, a detailed analysis of the molecular conformation or packing properties and the relationship between the structure and μ_{FET} of these fluorene-based thiophene oligomers have not been reported, except for a few papers on a structure analysis of thiophene−biphenyl co-oligomers.[13] The structural analysis of single crystals containing fluorene units would be very meaningful because this unit is a basic building block of polyfluorenes, one of the most promising and popular structures that are employed in various fields of organic electronics and photonics, as mentioned above.

In the present paper, we report on high performance and stable p-type active materials for OFETs based on a structural combination of a fused bithiophene with fluorene (BFTT) or biphenyl units (BPTT), and the structure−electrical property relationship in these materials. The two molecules have almost identical molecular structures, the only difference being a fluorene unit in BFTT from a biphenyl unit in BPTT. However, the findings herein demonstrate that this small difference in molecular structure led to substantial differences for two important electrical properties, that is, μ_{FET} and device stability. A 1.5−2 times higher μ_{FET} was achieved in the case of the biphenyl end-capped fused bithiophene, BPTT, compared to the fluorene end-capped derivative, BFTT. This mobility difference could be explained by the difference in molecular conformations and packing properties in their single crystals. In addition, BPTT-based devices showed a better air and UV stability than BFTT-based devices. The better air stability of BPTT OFETs could be explained by a relatively low HOMO level of BPTT which can avoid increase of off current of the device by oxidation doping, and the poor UV stability of the BFTT OFET could be explained by keto-defect formation in fluorene units via photooxidative reactions.

Results and Discussion

Molecular Conformation and Packing in a Single Crystal. The chemical structures of BFTT, BPTT, and FTTF

(3) (a) Fichou, D. *J. Mater. Chem.* **2000**, *10*, 571. (b) Fichou, D.; Bachet, B.; Demanze, F.; Billy, I.; Horowitz, G.; Garnier, F. *Adv. Mater.* **1996**, *8*, 500. (c) Siegrist, T.; Christian, K.; Laudise, R. A.; Katz, H. E.; Haddon, R. C. *Adv. Mater.* **1998**, *10*, 379. (d) Antolini, L.; Horowitz, G.; Kouki, F.; Garnier, F. *Adv. Mater.* **1998**, *10*, 382. (e) Li, X.-C.; Sirringhaus, H.; Garnier, F.; Holmes, A. B.; Moratti, S. C.; Feeder, N.; Clegg, W.; Teat, S. J.; Friend, R. H. *J. Am. Chem. Soc.* **1998**, *120*, 2206. (f) Antonio, F.; Yoon, M.-Y.; Stern, C. L.; Katz, H. E.; Marks, T. J. *Angew. Chem., Int. Ed.* **2003**, *42*, 3900. (g) Koren, A. B.; Curtis, M. D.; Kampf, J. W. *Chem. Mater.* **2000**, *12*, 1519. (h) Bader, M. M.; Custelcean, R.; Ward, M. D.; *Chem. Mater.* **2003**, *15*, 616. (i) Cornil, J.; Beljonne, D.; Calbert, J. P.; Bredas, J. L. *Adv. Mater.* **2001**, *13*, 1053.

(4) (a) Koren, A. B.; Curtis, M. D.; Francis, A. H.; Kampf, J. W. *J. Am. Chem. Soc.* **2003**, *125*, 5040. (b) Curtis, M. D.; Cao, J.; Kampf, J. W. *J. Am. Chem. Soc.* **2004**, *126*, 4318 (c) Mas-Torrent, M.; Hadley, P.; Bromley, S. T.; Ribas, X.; Tarres, J.; Mas, M.; Molins, E.; Veciana, J.; Rovira, C. *J. Am. Chem. Soc.* **2004**, *126*, 8546.

(5) Müller, K.; Wegner, G. *Electronic Materials: The Oligomer Approach*; Wiley-VCH: New York, 1998.

(6) (a) *Handbook of Oligo- and Polythiophenes*; Fichou, D., Ed.; Wiley-VCH: Weinheim, Germany, 1999. (b) Gundlach, D. J.; Lin, Y.-Y.; Jackson, T. N.; Schlom, D. G. *Appl. Phys. Lett.* **1997**, *71*, 3853.

(7) Barbarella, G.; Zambianchi, M.; Bongini, A.; Antolini, L. *Adv. Mater.* **1993**, *5*, 834.

(8) (a) Hotta, S.; Waragai, K. *J. Mater. Chem.* **1991**, *1*, 835. (b) Liao, J.-H.; Benz, M.; Legoff, E.; Kanatzidis, M. G. *Adv. Mater.* **1994**, *6*, 135. (c) Horowitz, G.; Bachet, B.; Yassar, A.; Lang, P.; Demanze, F.; Fave, J.-L.; Garnier, F. *Chem. Mater.* **1995**, *7*, 1337. (d) Pelletier, M.; Brisse, F. *Acta Crystallogr., Sect. C* **1994**, *50*, 1942. (e) Graf, D. D.; Duan, R. G.; Campbell, J. P.; Miller, L. L.; Mann, K. R. *J. Am. Chem. Soc.* **1997**, *119*, 5888. (f) Dicesare, N.; Belletete, M.; Garcia, E. R.; Leclerc, M.; Durocher, G. *J. Phys. Chem. A* **1999**, *103*, 3864. (g) Mitschke, U.; Osteritz, E. M.; Debaerdemaeker, T.; Sokolowski, M.; Bäuerle, P. *Chem.−Eur. J.* **1998**, *4*, 2211. (h) Azumi, R.; Goto, M.; Honda, K.; Matsumoto, M. *Bull. Chem. Soc. Jpn.* **2003**, *76*, 1561.

(9) (a) Katz, H. E.; Bao, Z.; Gilat, S. L. *Acc. Chem. Res.* **2001**, *34*, 359. (b) Garnier, F.; Hajlaoui, R.; Yassar, A.; Srivastava, P. *Science* **1994**, *265*, 1684.

(10) Hong, X. M.; Katz, H. E.; Lovinger, A. J.; Wang, B.-C.; Raghavachari, K. *Chem. Mater.* **2001**, *13*, 4686.

(11) (a) Meng, H.; Bao, Z.; Lovinger, A. J.; Wang, B.-C.; Mujsce, A. M. *J. Am. Chem. Soc.* **2001**, *123*, 9214. (b) Meng, H.; Zheng, J.; Lovinger, A. J.; Wang, B.-C.; Patten, P. G. V.; Bao, Z. *Chem. Mater.* **2003**, *15*, 1778.

(12) (a) Neher, D. *Macromol. Rapid Commun.* **2001**, *22*, 1365. (b) Scherf, U.; List, E. J. W. *Adv. Mater.* **2002**, *14*, 477. (c) List, E. J. W.; Guentner, R.; de Freitas, P. S.; Scherf, U. *Adv. Mater.* **2002**, *14*, 374.

(13) (a) Hotta, S.; Goto, M. *Adv. Mater.* **2002**, *14*, 498. (b) Hotta, S.; Goto, M.; Azumi, R.; Inoue, M.; Ichikawa, M.; Taniguchi, Y. *Chem. Mater.* **2004**, *16*, 237.

Scheme 1. Chemical Structures and Abbreviations Investigated in This Work

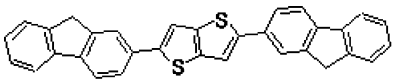

BFTT

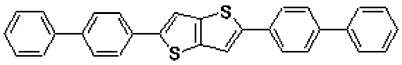

BPTT

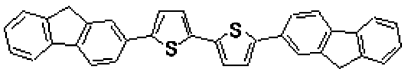

FTTF

Table 1. Crystal Data and Structure Refinement for BFTT and BPTT

	BFTT	BPTT
empirical formula	$C_{32}H_{20}S_2$	$C_{30}H_{20}S_2$
formula weight	468.60	444.58
temperature (K)	253(2)	253(2)
crystal system	triclinic	monoclinic
space group	$P\bar{1}$	$P2_1/a$
a (Å)	5.767 6(11)	8.007 7(8)
b (Å)	8.536 9(16)	5.640 2(5)
c (Å)	22.949(4)	23.749(2)
α (deg)	100.272(4)	90
β (deg)	94.846(3)	99.215(2)
γ (deg)	92.070(4)	90
V (Å^3)	1106.3(4)	1058.78(17)
Z	2	2
crystal size (mm)	0.48 × 0.48 × 0.01	0.40 × 0.40 × 0.01
color of crystal	yellow	pale yellow
D_{calcd} (g/cm^3)	1.407	1.395
radiation	Mo Kα	Mo Kα
θ range (deg) for data collection	0.91−28.35	0.87−28.40
range of h, k, l	$-7 \le h \le 5$ $-8 \le k \le 11$ $-29 \le l \le 30$	$-9 \le h \le 10$ $-7 \le k \le 3$ $-31 \le l \le 31$
no. reflections measured	7303	6806
no. unique reflections	5119	2588
no. reflections used	3902 [$I > 2\Sigma(I)$]	2588 [$I > 2\Sigma(I)$]
no. parameters	345	164
goodness of fit	1.166	0.960
R1 [$I > 2\Sigma(I)$]	0.0694	0.0470
wR2	0.2069	0.1266
largest diff. peak and hole (e·Å^{-3})	0.302 and −0.327	0.259 and −0.266

used in this study are shown in Scheme 1. FTTF was prepared to compare OFET device performance by means of a known procedure.[11] The only structural difference between the two molecules, BFTT and BPTT, is a biphenyl and fluorene unit, located at both ends of those molecules, respectively. Thus, any difference in properties could be directly correlated with this structural dissimilarity. The crystal data and structure refinement for BFTT and BPTT are summarized in Table 1. The BFTT crystals belong to the triclinc space group $P\bar{1}$, whereas those of BPTT belong to the monoclinic space group $P2_1/a$, the same as the crystal system of BPnT (biphenyl thiophene derivatives),[13b] which have almost the same molecular structure except the fused bithiophene in the core of the oligomer.

Figure 1a,b shows ORTEP drawings of BFTT and BPTT with the atomic numbering scheme, respectively. The inner thiophene planes in the fused thiophene unit for both molecules have an all-anti conformation with a perfect planar structure of a zero dihedral angle between each thiophene unit and are disordered with the possibility of about 60% for the S1 and S1a conformation and 40% for the S1A and S1Aa conformation, respectively. This zero dihedral angle is different from the dihedral angle between the inter-thiophene rings of all unsubstituted oligothiophenes having a small dihedral angle.[3a]

Two crystallographically independent molecules (form A and form B) were obtained in the unit cell of BFTT. Both form A and form B have a center of symmetry. We can easily recognize the different molecular conformations with different torsional and bending angles via a side view of the ORTEP representation. Form A of BFTT exhibits a very planar molecular structure with small torsional angles, different from that of form B. The calculated dihedral angle between the least-squares planes (LSPs) of fluorene and fused bithiophene in form A is 0.2°. This small torsional angle between the inter-rings indicates a quasi-planar structure and is comparable with the reported dihedral angle for the unsubstituted even-number oligothiophene (∼1°) or *p*-sexiphenyl (3.3−3.6°).[3a,14] On the other hand, the form B of BFTT shows the zigzag shape with a larger dihedral angle, as shown in the side ORTEP view of Figure 1. The calculated dihedral angle between the LSPs of fluorene and fused thiophene in form B is 10°. Those different conformations of the two forms of BFTT resulted from the presence of C7 and C23, that is, the carbon at the 9 position of the fluorene unit in BFTT and the hydrogens attached to it, which are the only differences between BFTT and BPTT.

Contrary to the results of BFTT, BPTT crystal affords only one conformer with a center of symmetry. All dihedral angles between LSPs of aromatic rings of BPTT show a quite small value below 2.5°. The dihedral angle between the benzene rings of the biphenyl moiety is 2.2°, indicating an almost coplanar conformation. Those angles are also in good agreement with the reported dihedral angle of a pair of adjacent benzene rings of oligophenylenes or BP1T.[13a]

The bending angles between the molecular segments (fluorene, biphenyl, and fused thiophene) of BFTT and BPTT were also compared. To calculate the bending angles, two forms of BFTT and BPTT molecules are divided into three straight segments, composed of a fluorene or a biphenyl unit and the bithiophene core, respectively. To identify these segments, the segment axes are defined as the lines, namely, C1−C12 and C17−C28 (fluorene unit of forms A and B, respectively) and C14−C14a and C30−C30b (fused bithiophene unit) for BFTT. As for BPTT, C1−C10 (biphenyl unit) and C13−C13a (fused bithiophene unit) are employed as segment axes. For the two forms of BFTT, form B also shows a larger bending angle between the fluorene and the bithiophene unit than form A. The calculated bending angles between fluorene, that is, C1−C12 and C17−C28, and bithiophene, that is, C14−C14a and C30−C30b, for forms A and B in BFTT were 10.6 and 14.3°, respectively. The

(14) Baker, K. N.; Fratini, A. V.; Resch, T.; Knachel, H. C.; Adams, W. W.; Socci, E. P.; Farmer, B. L. *Polymer* **1993**, *34*, 1571.

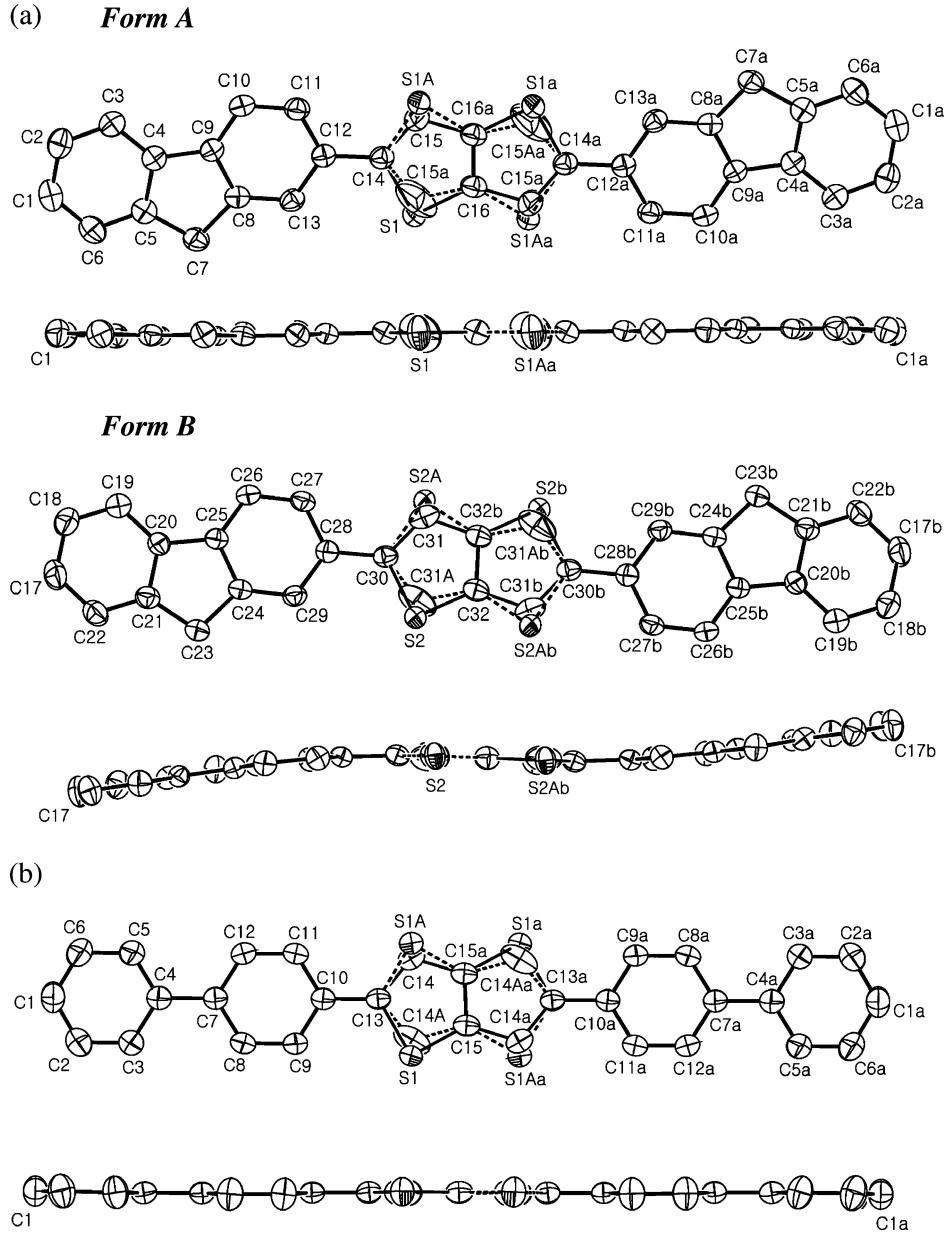

Figure 1. ORTEP front views and side views of (a) BFTT and (b) BPTT with the atomic numbering scheme. Displacement ellipsoids are drawn at the 50% probability level.

calculated bending angle between biphenyl, that is, C1−C10, and bithiophene, C13−C13a, in BPTT is about 0.2° indicating a very small value. Those small dihedral and bending angles in BPTT led to its almost planar and straight shape.

Figures 2 and 3 show packing diagrams of BFTT and BPTT, respectively. These molecules form the well-known herringbone packing extending along the *ab* plane.[3a] The herringbone angles of BFTT and BPTT were determined from the dihedral angle between the LSPs of the nearest neighbors including all non-hydrogen atoms in one molecule. The calculated herringbone angles based on such a definition of BFTT and BPTT are 61.2 and 65.2°, respectively, which are similar to that for nonsubstituted α-6T[6a] or biphenyl/thiophene co-oligomer, that is, BP*n*T.[13b] The difference in herringbone angles between BFTT and BPTT might be also induced from C7 and C23, that is, the carbon at the 9 position of the fluorene unit in BFTT and the hydrogens attached to it. The tilting angles were also calculated between the molecular long axis, which is defined as the line vector of C1−C1a, and normal to the *ab* plane. The computed tilting angles for BFTT and BPTT are 21 and 18°. The tilting angles are larger than those of BP*n*T, which have a similar component and show extremely small tilting angles (1.2° in the case of BP2T, biphenyl end-capped unfused bithiophene) but smaller than those of all other unsubstituted oligothiophenes.[3a,13b] The fused thiophene structure of the BPTT resulted in a molecular structure with a planar conformation, instead of a zigzag conformation, and also could cause a larger density of BPTT (1.395 g/cm^3) than that of unfused BP2T (1.373 g/cm^3).[13b] Interestingly, these results demonstrate that quite important differences in molecular properties such as electronic properties could be induced simply by whether the thiophene ring is fused (BPTT) or not (BP2T).

Figure 4a,b shows a projection view of the single-crystal structures of BFTT and BPTT, respectively, along the

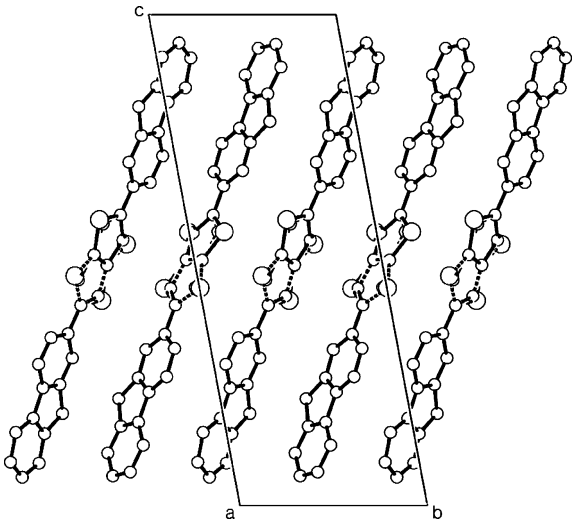

Figure 2. Projection view of BFTT along the *a* axis.

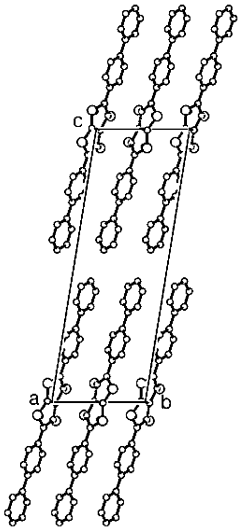

Figure 3. Projection view of BPTT along the *a* axis.

molecular long axis. The single crystal of BFTT was composed of two unique conformations of forms A and B as noted in Figure 4a. The four hydrogens bonded at C7 and C7a in the fluorene unit of form A of BFTT stretch out symmetrically from the main plain of the molecule with a bonding angle of 109.09°. Thus, the angle of curvature between the main LSPs of BFTT and each hydrogen is 54.545°. On the other hand, the hydrogens bonded at C23 and C23b in the fluorene unit of form B of BFTT stretch out unsymmetrically and are distorted, to a certain extent. The distortion is easily observed in Figure 4a and is consistent with the relatively large dihedral angle in the main LSPs of BFTT previously mentioned. The perpendicular thiophene or phenylene dimers have larger attractive interaction energies than the parallel dimers.[15] The large interaction energy is the cause of the preference for the herringbone structure in the crystals of nonsubstituted oilgothiophenes or oligophenylenes. Here, the same interaction exists leading to the herringbone structure; however, the hydrogen atoms at the 9-position carbon stretching out of the fluorene plane in form A cause some steric pressure, leading to the conformational strain of form B. On the contrary, the molecules of BPTT in the single crystal are packed as a unique molecular conformation with a unit cell lengths of $a = 8.007\,7(8)$ Å and $b = 5.640\,2(5)$ Å. The length of the unit cells of BPTT is slightly smaller than that of BFTT, that is, $a = 5.767\,6(11)$ Å and $b = 8.536\,9(16)$ Å.

The shortest intermolecular distances were also calculated (see Supporting Information). The shortest intermolecular distances of sulfur-to-sulfur, sulfur-to-carbon, and carbon-to-carbon in the BFTT single crystal are 3.566(8) (S1A−S2), 3.478(4) (S1−C28) and 3.423(5) Å (C8−C23), respectively, and all contacts are almost the same or larger than the sum of the van der Waals radii involving sulfur (1.8 Å) or carbon (1.7 Å). However, the shortest intermolecular distances of those in the BPTT single crystal are slightly less than those of BFTT such as 3.399(2) Å (S1−C14). The other intermolecular distances also follow this trend, and this result also indicates that BPTT molecules in the single crystal have better packing properties with a larger overlap of intermolecular π orbitals than BFTT.

Even though it is known that some difference may exist between the thin film polycrystalline phase and the single-crystal phase of organic semiconductors, in these two phases, the same crystal packing is involved in terms of intra- and intermolecular forces.[1c] Therefore, many research groups have used the results of a single-crystal analysis to identify the mobility properties of OFETs in a polycrystalline phase fabricated from organic semiconducting materials.[3] Actually, two major parameters, that is, the intensity of electron coupling between adjacent molecules and the reorganization energy, should be considered to precisely determine the difference in charge mobility among organic semiconductors.[16] However, an interesting report from Torrent et al. showed that the charge carrier mobility can also be readily estimated from the difference in the crystal structure and the packing characteristics among molecules if they have similar moieties because the two major parameters are also strongly correlated with crystal structure.[4c] On the basis of these findings, we used the results of the single-crystal analysis described earlier to explain differences in the electrical properties of fluorene/thiophene (BFTT) and biphenyl/thiophene co-oligomers (BPTT).

Structural Investigations on Thin Films. An atomic force microscope (AFM) was used to observe the morphology of the active layer materials, which were deposited on thermally grown silicon dioxide (SiO_2). The surface of the substrate was pretreated with 1,1,1,3,3,3-hexamethyldisilazane (HMDS) to reduce the surface energy between the oligomers and the SiO_2 interface. Figure 5a−d shows AFM images of BPTT and BFTT thin films (∼50 nm thick) deposited on SiO_2, at 100 and 150 °C, respectively. As shown in Figure 5b,d and their height profiles (not shown), it was clear that both films show a layered morphology with the smallest terrace step size of 2.2−2.3 nm, consistent with the

(15) Tsuzuki, S.; Honda, K.; Azumi, R. *J. Am. Chem. Soc.* **2002**, *124*, 12200.

(16) (a) Gruhn, N. E.; da Silva Filho, D. A.; Bill, T. G.; Malagoli, M.; Coropceanu, V.; Kahn, A.; Brédas, J. L. *J. Am. Chem. Soc.* **2002**, *124*, 7918. (b) Bromley, S. T.; Mas-Torrent, M.; Hadley, P.; Rovira, C. *J. Am. Chem. Soc.* **2004**, *126*, 6544.

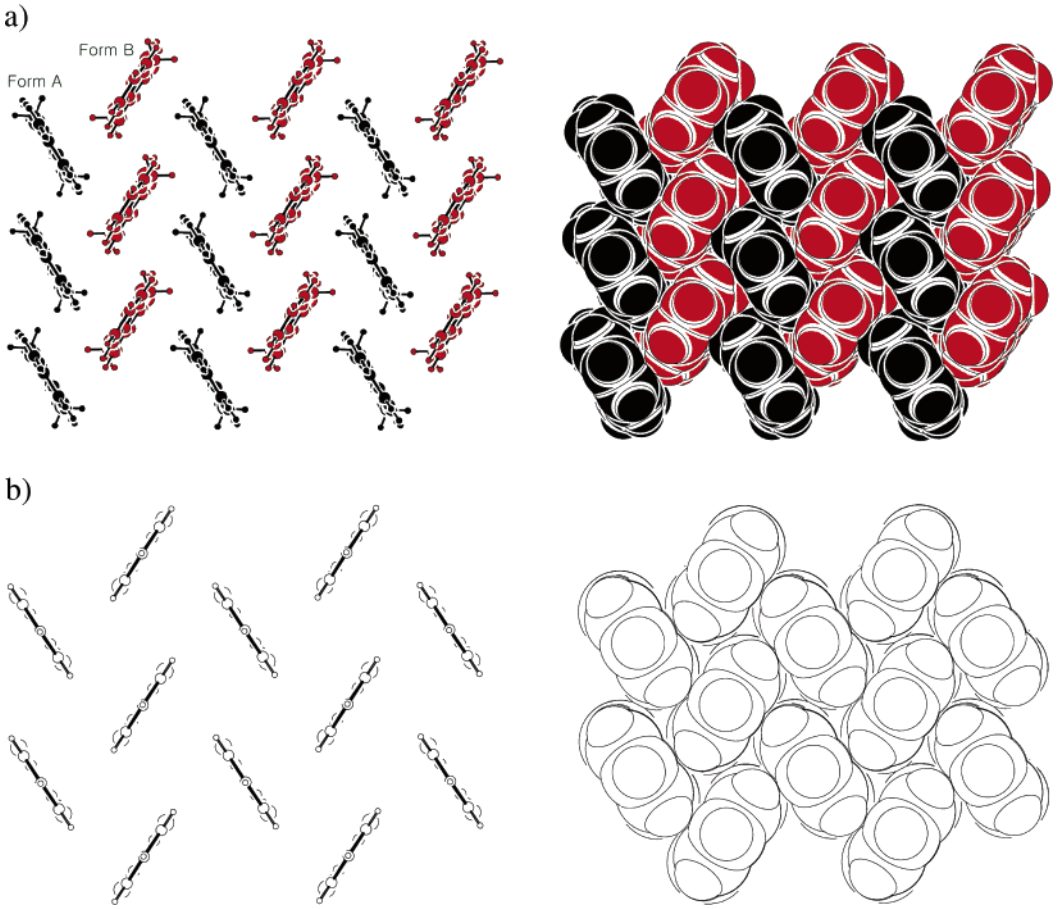

Figure 4. Packing diagram of (a) BFTT and (a) BPTT viewed along the long axis of the molecule.

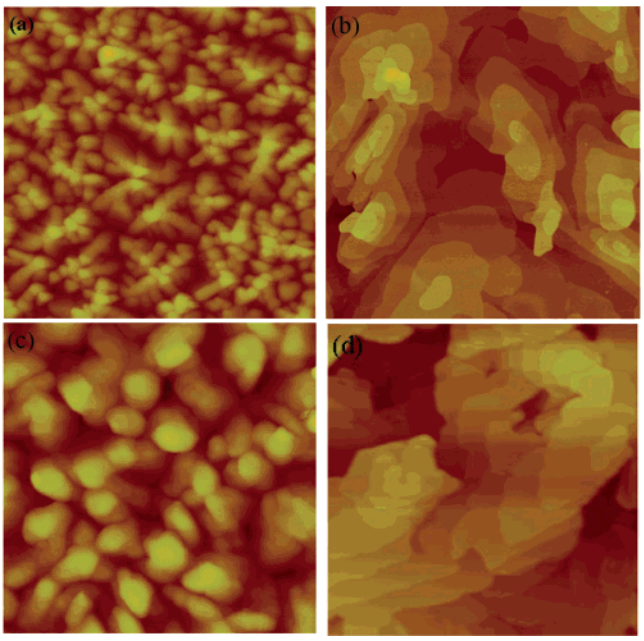

Figure 5. AFM images of films deposited on SiO_2 at various T_S values. (a) BPTT, 4 μm × 4 μm (T_S = 100 °C); (b) BPTT, 10 μm × 10 μm (T_S = 150 °C); (c) BFTT, 4 μm × 4 μm (T_S = 100 °C); (d) BFTT, 10 μm × 10 μm (T_S = 150 °C).

size of the long axis of the oligomers (Table 1), when grown at a substrate temperature (T_S) above 150 °C. Both thin films of oligomers showed a quite similar grain size with a spherical shape, when deposited on a room-temperature substrate (not shown). The grain size of the films was enlarged, when the T_S in the BPTT and BFTT films increased as shown in Figure 5. No significant difference in morphologies was noted between the two samples in terms of grain size and shape at every T_S. This suggests that no major difference in the number density of intergrain in the same channel area is evident between the source and the drain electrodes. Therefore, any effect of grain size or the density of the grain boundary on the carrier mobility difference between two molecules can be excluded.[17]

The orientation of the thin films was investigated by means of X-ray diffraction (XRD) analysis. Figure 6a,b shows X-ray diffractograms of BPTT and BFTT films (~50 nm) deposited on SiO_2/Si at T_S = room temperature, 50, 100, 150, and 175 °C. X-ray diffractograms of BPTT and BFTT films show a high degree of ordering with sharp reflection peaks, which corresponds to the length of the long axis of the molecules or its long-range orders. The first reflection peak for BPTT at 3.8° (d = ca. 2.3 nm) was observed at a slightly shorter diffraction angle than that for BFTT at 3.95° (d = ca. 2.2 nm). This result is consistent with the results of the lattice constants obtained from the single-crystal analysis, as shown in Table 1. This indicates that, compared to BFTT, BPTT has a slightly longer molecular length as a molecular conformation or a slightly longer unit in the thin films along the direction normal to the substrate, because the biphenyl

(17) (a) Horowitz, G.; Hajlaoui, M. E. *Adv. Mater.* **2000**, *12*, 1046. (b) Kelley, T. W.; Frisbie, C. D. *J. Phys. Chem. B* **2001**, *105*, 4538. (c) Street, R. A.; Knipp, D.; Völkel, A. R. *Appl. Phys. Lett.* **2002**, *80*, 1658. (d) Verlaak, S.; Arkhipov, V.; Heremans, P. *Appl. Phys. Lett.* **2003**, *82*, 745.

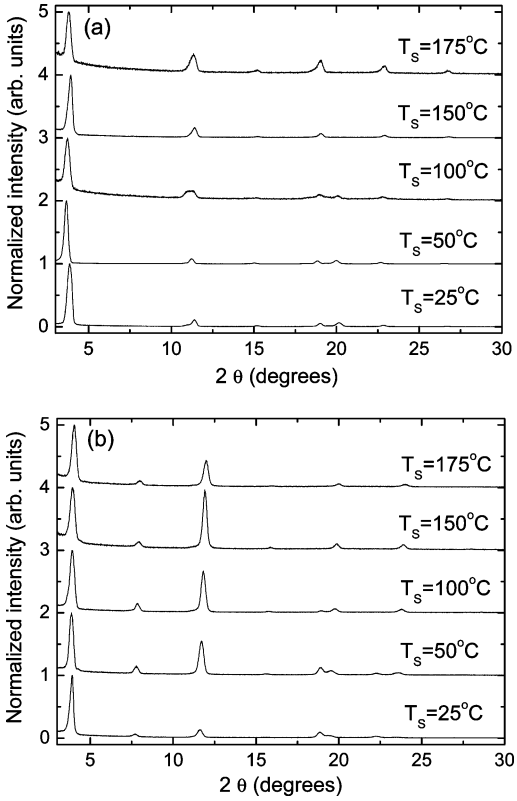

Figure 6. X-ray diffractograms of (a) BPTT and (b) BFTT films (~50 nm) deposited on SiO_2 at T_S = room temperature, 50, 100, 150, and 175 °C.

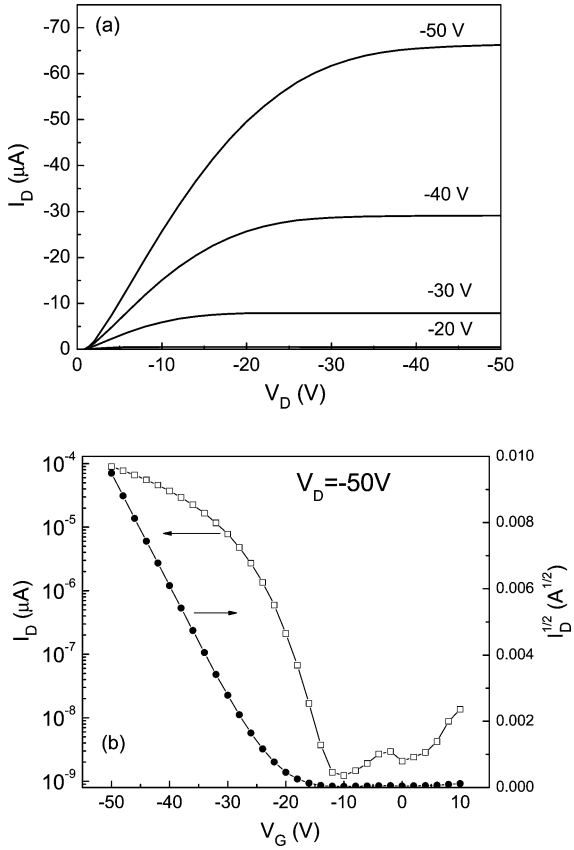

Figure 7. (a) Drain current (I_D) versus drain-source voltage (V_D) characteristics of the BPTT OFET at different gate voltages (V_G). The gate voltage was varied from 0 to −50 V in steps of −10 V. (b) I_D versus V_G characteristics of the BPTT OFET at a drain current of −50 V.

unit has a quasi-planar and straight structure with almost zero bending and dihedral angles compared to the fluorene unit with relatively large bending and dihedral angles (form B). The values for the calculated *d* spacing from the first reflection peaks of both molecules were almost the same as the step heights of terraced islands, as measured by the AFM as shown in Figure 5b,d. These results demonstrate that both molecules are oriented in the same manner; that is, the long-axis of the molecules lie closely in the direction normal to the substrate. This suggests that films deposited at T_S = 150 °C would show a layered morphology with an edge-on orientation. Such a film morphology is known to be a favorable structure in polycrystalline films in terms of achieving a high mobility.[1] One interesting note is the absence of (002) peak in the XRD pattern of the BPTT thin films as shown in Figure 6a. A reproducible absence of this peak for all samples is not likely due to the deficiency of symmetry of the thin-film unit cell but structure factor considerations because other higher ordered (00*l*) peaks were observed in the BPTT thin films.[18]

Characteristics of OFETs. OFETs of BPTT, BFTT, and FTTF with a top-contact configuration were fabricated to measure various performances, such as charge carrier mobility, I_{ON}/I_{OFF}, and threshold voltage (V_{TH}). Figure 7a,b shows the drain current (I_D) versus source-drain voltage (V_D) or gate voltage (V_G) characteristics with various V_G values for the p-channel OFETs of BPTT deposited at T_S = 150 °C, respectively. All top-contact devices using BPTT, BFTT, and FTTF as the active layer showed well-defined linear and saturation characteristics, as shown in Figure 7a. The μ_{FET} and V_{TH} of the OFETs were obtained from eq 1 for saturation regimes.[1a]

$$I_D^{sat} = (W/2L)\mu_{FET}C_i(V_G - V_{TH})^2 \quad (1)$$

where *L* is the channel length, *W* is the channel width, and C_i is the capacitance per unit area of the gate dielectric layer (C_i = 10 nF/cm² for 300 nm thick SiO_2). The calculated μ_{FET}, I_{ON}/I_{OFF}, and V_{TH} of the BPTT device by plotting I_D and $I_D^{1/2}$ versus V_G were 0.093 $cm^2\ V^{-1}\ s^{-1}$, 7.3×10^4, and −22 V, respectively, as shown in Figure 7b.

The performances of other devices with the active layers deposited at various T_S values, prepared from other compounds, are summarized in Table 2. OFETs for *unsubstituted* FTTF as the active layer were also fabricated to compare the results obtained here with previous results reported from other groups. The μ_{FET} and I_{ON}/I_{OFF} measured in our laboratory were almost the same as previously reported data.[11a] The shift in V_{TH} with T_S can be explained by a lowering of contact resistance via a better packing with increase of T_S.[19] The μ_{FET} of devices using biphenyl-based BPTT as the active layer showed a 1.5−2 times higher value than that from fluorene-based BFTT and FTTF at the same T_S. These results are quite consistent with the single-crystal

(18) Merlo, J. A.; Newman, C. R.; Gerlach, C. P.; Kelly, T. W.; Muyres, D. V.; Fritz, S. E.; Toney, M. F.; Frisbie, C. D. *J. Am. Chem. Soc.* **2005**, *127*, 3997.
(19) Horowitz, G.; Hajlaoui, M. E.; Hajlaoui, R. *J. Appl. Phys.* **2000,** *87*, 4456.

Table 2. OFET Characteristics of Oligomers Fabricated at Different T_S Values[a]

material	T_S [°C]	μ_{FET} [$cm^2 V^{-1} s^{-1}$]	V_{TH} [V]	I_{ON}/I_{OFF}
BPTT	25	0.02−0.03 (0.02−0.03)	−36 (−21)	8400 (8100)
	100	0.07−0.08 (0.06−0.07)	−32 (−22)	6×10^4 (6×10^4)
	150	0.08−0.09	−22	7.3×10^4
BFTT	25	0.01−0.02 (0.009−0.01)	−30 (−20)	4500 (4000)
	100	0.04−0.05	−21	4×10^4
	150	0.05−0.06 (0.02−0.03)	−24 (−24)	7×10^4 (4.5×10^4)
FTTF	150	0.05−0.06 (0.02−0.03)	−19 (−18)	6.3×10^4 (3.2×10^4)

[a] Values in parentheses were measured using the same devices after about 1 month.

analysis mentioned above: both a shorter intermolecular distance and uniform and planar molecular structure in the case of BPTT crystals. Other factors which influence μ_{FET} such as grain size or the size of the gap between grains can be excluded, because the films from both molecules showed an almost identical grain size and morphology. Therefore, we can conclude that a difference in the conformation of the molecules and the packing characteristics, which were induced from the structural difference between fluorene and biphenyl units, leads to this difference in μ_{FET}. The hydrogens bonded to carbon at the 9 position in the fluorene unit of BFTT would hinder the formation of a close-packed structure, which has an increased intermolecular overlap of electronic wave functions, because the hydrogens of BFTT at the 9 position are oriented in almost the same direction with the main overlap direction between the π orbitals of the nearest neighbor molecules having a herringbone packing. On the contrary, the biphenyl structure could have sufficient planarity for a close intermolecular packing in the solid film with a very small torsional angle, as reported by Hotta et al.[13] Although the reorganization energy, which can have an effect on μ_{FET},[4c] was not considered in reaching this conclusion, we expect that the difference in reorganization energies between BPTT and BFTT is small, because the molecular structures of the two molecules are very similar.

The performances of the selected devices were measured again after about 1 month of storage under ambient dark conditions for an air stability test. The BPTT devices that were measured 1 month later showed almost the same or a slightly decreased μ_{FET} and I_{ON}/I_{OFF} without an off current increase, as shown in Table 2. All the BPTT devices measured after 1 month showed a value that was above 80% of the original μ_{FET}. One interesting finding was that the threshold voltage decreased considerably in the devices measured after 1 month. The same behavior was reported for a methanofullerene (PCBM) device prepared by Waldauf et al.[20] This behavior might be induced by a slight filling of the trap site. On the contrary, the BFTT or FTTF devices stored for 1 month showed half of the original μ_{FET} and a decreased I_{ON}/I_{OFF} because of a slight increase in the off current. This instability of the BFTT and FTTF devices can be attributed to a relatively higher HOMO energy level of the fluorene-based oligomers, BFTT and FTTF, than that of the biphenyl based oligomer, BPTT. The HOMO energy levels were measured to investigate the possible effects of this HOMO level difference on the air stability of the devices. Figure 8 and the inset show cyclic voltammetry (CV) data for BPTT and BFTT films on indium tin oxide (ITO)-coated glass. Both films showed reversible oxidation and a reduction sweep implying the stable formation of a radical cation and anion state, respectively. The measured HOMO energetic levels of these molecules by CV and ultraviolet photoelectron spectroscopy (UPS), including optical band gaps, are summarized in Table 3. Both BFTT and FTTF, fluorene-based molecules, showed HOMO energy levels of 5.3−5.4 eV, and these values were confirmed by both methods. The HOMO energy level of BPTT, 5.5 eV, was slightly lower than those for BFTT and FTTF. Therefore, this lower HOMO level of BPTT might have led to a better air stability of the OFETs because there would be less probability of oxygen doping in the case of a BPTT.[9] The absorption spectra of both films showed that BPTT and BFTT have an almost similar band gap (see Supporting Information).

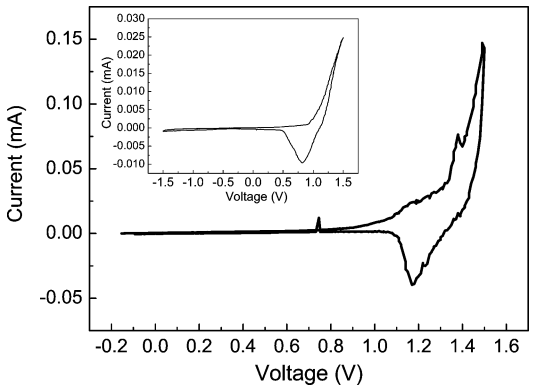

Figure 8. Cyclic voltagmmogram of the BPTT film or BFTT film (inset) on ITO-coated glass.

Table 3. HOMO Energy Levels and Band Gaps of Oligomers

material	oxidation E_{onset} (V) HOMO (eV)	HOMO[a] (eV)	oxidation E_{pa}/E_{pc} (V)	λ_{onset} (nm) E_g (eV) UV[b]
FTTF[c]	0.92		1.12/0.82	468
	5.36			2.65
BFTT	0.95		1.25/0.75	465
	5.39	5.3		2.67
BPTT	1.02		1.37/1.17	465
	5.46	5.5		2.67

[a] HOMO energy levels are measured by UPS measurement. [b] HOMO and LUMO gaps (E_g) are measured according to the onset of UV absorption of the films. [c] The values for FTTF are obtained from ref 11a.

Some of the devices were measured after UV irradiation to check for UV stability. This experiment is a type of an accelerated test for photo- or thermal-oxidative degradation of organic semiconductor materials. If OFETs have been operated in air under ambient sunlight or at a slightly high temperature, it would be expected that these accelerated tests would provide interesting and useful information on the stability issues. BFTT (T_S = 150 °C) and BPTT (T_S = 50 °C) devices were fabricated as described in the experimental section and measured immediately (fresh) or after UV

(20) Waldauf, C.; Schilinsky, P.; Perisutti, M.; Hauch, J.; Brabec, C. J. *Adv. Mater*. **2003**, *15*, 2084.

Table 4. BFTT (T_S = 150 °C) and BPTT (T_S = 50 °C) OFET Characteristics before and after UV Irradiation in Air or a Nitrogen Atmosphere[a]

	μ_{FET} [cm²/V·s]	V_{TH} [V]	S.S [V/dec]	I_{ON}/I_{OFF}	I_{OFF} [A]
			BFTT		
fresh	0.053	−23.4	3.5	77 000	9.0×10^{-10}
	(0.037)	(−27)	(4.5)	(53 000)	(3.5×10^{-9})
3 h later	0.012	−22.9	4.1	14 000	1.3×10^{-9}
	(0.023)	(−25.4)	(4.6)	(42 000)	(3.4×10^{-9})
6 h later	0.0021	−29.6	6.1	1400	1.0×10^{-9}
	(0.017)	(−21.8)	(5)	(40 000)	(3.5×10^{-9})
			BPTT		
fresh	0.039	−23.9	3.2	55 000	1.1×10^{-9}
3 h later	0.024	−16.4	3.7	43 000	2.7×10^{-9}
6 h later	0.014	−15.1	4.8	17 000	3.8×10^{-9}

[a] Values in parentheses were measured with BFTT OFETs, which had been deposited on an untreated SiO_2 surface with HMDS, before and after UV irradiation in a nitrogen atmosphere.

irradiation for 3 h and 6 h. The measured and calculated device performances are summarized in Table 4.

The BFTT device showed a more rapid degradation in performance after UV irradiation in air. The μ_{FET} value for the BFTT device, after UV irradiation in air for 6 h, decreased to a value about 20 times smaller than that of a fresh device. However, the BPTT device in air or the BFTT device in nitrogen, even after UV irradiation for 6 h, showed a relatively smaller decrease in μ_{FET} (∼50%). Another notable feature of the degradation of the BFTT device after UV irradiation in air was an increase in switch-on voltage or V_{TH}. The BFTT device, after irradiation under a UV lamp for 6 h in air, showed a large increase in V_{TH} from −23.4 V to −29.6 V. The increase in V_{TH} is believed to be due to a contribution by keto-defect formation in the fluorene unit of the BFTT under UV irradiation[21] because the V_{TH} value depends on the density of the trap following the multiple trap released (MTL) model proposed by Horowitz et al.[1a] A number of traps would be generated in the band gap via the formation of keto-defects, and more charge carriers would then be required to fill the increased trap sites. Therefore, a higher V_G would be required to obtain an effective current flow in the conduction or valence band region. The increased concentration in trap states as the result of keto-defects is also supported by the slightly larger difference in calculated mobility values between the saturation and linear regime, for the case of the device measured after UV irradiation for 6 h in air, compared to the fresh and devices that had been irradiated in air for 3 h.[1c] The fact that a clear increase in V_{TH} was observed after a 6 h period of UV irradiation is also consistent with the Fourier transform infrared (FT-IR) transmission spectra of BFTT and BPTT films (∼300 nm thick). Figure 9 shows the FT-IR transmission spectra of the BFTT and BPTT films before and after UV irradiation for 6 h in air. The 300 nm thick films for FT-IR measurement were prepared on SiO_2/Si by thermal evaporation in a high vacuum chamber. The thickness of the BFTT and BPTT film was checked by a thickness monitor with quartz crystal. The baselines of measured data were corrected manually by software of a Perkin Elmer 2000 FT-IR. The BFTT film showed a clearly visible peak at 1721 cm^{-1} corresponding to the carbonyl stretching (>C═O) mode due to the formation of keto-defects after UV irradiation for 6 h. On the other hand, no carbonyl stretching peak was observed for the BPTT film even after UV irradiation for 6 h. This confirms that this degradation can be attributed to the formation of keto-defects. The formation of a keto-defect in the BFTT film was also confirmed by the change of the photoluminescence (PL) spectra after UV irradiation (see Supporting Information). The intensity of the peaks at 540 nm (∼2.3 eV) and 585 nm (∼2.1 eV), corresponding to fluorenone emission, increased with UV irradiation time in the BFTT film.[12c] On the other hand, the intensity of the peak at 537 nm (∼2.3 eV) and 580 nm (∼2.1 eV) decreased with UV irradiation time in **the** BPTT film.

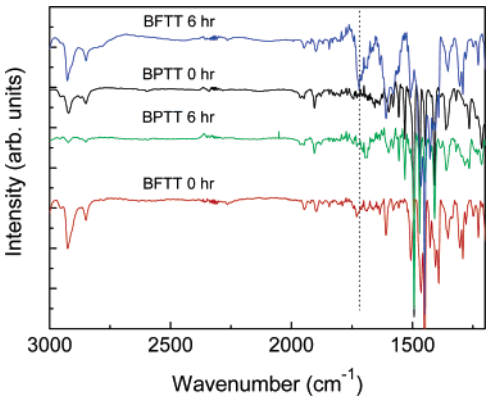

Figure 9. FT-IR transmission spectra of BFTT and BPTT films on SiO_2/Si before and after UV irradiation for 6 h in air.

Conclusions

In conclusion, using fused thiophene-, biphenyl-, and fluorene-based organic semiconducting oligomers, we systematically investigated the influence of a combination of molecular building blocks on their crystal structures and electrical properties, that is, charge carrier mobility and air and UV stability of OFETs. The biphenyl/fused-thiophene-based BPTT devices showed a 1.5−2 times higher μ_{FET} because the BPTT molecule has a more planar and straight conformation in the single crystal which can lead to a better packing motif than the fluorene/fused-thiophene-based BFTT molecule, which exists in two crystallographically independent conformations in one single crystal and has a more distorted structure. In addition, better air and UV stability were obtained for the BPTT devices than for the BFTT devices because of the lower HOMO energy levels of BPTT and the formation of keto-defects by the photo-oxidation in the BFTT film after UV irradiation. Thus, it was clearly demonstrated that even a slight change of the molecular structure from biphenyl to fluorene could lead to significant differences in device performance and stability. We expect further improvement on the performance and stability of OFETs in the near future via optimizing the molecular building blocks used.

(21) (a) List, E. J. W.; Guentner, R.; de Freitas, P. S.; Scherf, U. *Adv. Mater.* **2002**, *14*, 374. (b) Lupton, J. M.; Craig, M. R.; Meijer, E. W. *Appl. Phys. Lett.* **2002**, *80*, 4489. (c) Hintschich, S. I.; Rothe, C.; Sinha, S.; Monkman, A. P.; de Freitas, P. S.; Scherf, U. *J. Chem. Phys.* **2003**, *119*, 12017. (d) Gong, X.; Iyer, P. K.; Moses, D.; Bazan, G. C.; Heeger, A. J.; Xiao S. S. *Adv. Funct. Mater.* **2003**, *13*, 325 (e) Franco, I.; Tretiak, S. *Chem. Phys. Lett.* **2003**, *372*, 403.

Experimental Section

Synthesis. The BPTT and BFTT were synthesized using the Suzuki coupling reaction between 2,5-dibromothieno[3,2-b]thiophene[22] and the corresponding pinacolato boronic ester-substituted biphenyl and fluorene in close analogy to those described previously.[11a,23] Thermogravimetric analysis (TGA) and differential scanning calorimetry measurements were performed with a TA Instrument 2100 series under a nitrogen atmosphere at a heating rate of 5 °C/min. The decomposition temperature was determined at the onset point of weight loss by TGA.

2,5-Bis(4-biphenylyl)-thieno[3,2-b]thiophene (BPTT). Decomposition temperature determined by TGA: 347 °C. Elem anal. Calcd for $C_{30}H_{20}S_2$: C, 81.04; H, 4.53; S, 14.42. Found: C, 81.22; H, 4.53; S, 14.45.

2,5-Bis-(9H-fluorene-2-yl)-thieno[3,2-b]thiophene (BFTT). Mp 348 °C. Decomposition temperature determined by TGA: 396 °C. Elem anal. Calcd for $C_{32}H_{20}S_2$: C, 82.01; H, 4.30; S, 13.68. Found: C, 82.08; H, 4.42; S, 13.72.

Single-Crystal Structure. BPTT and BFTT were carefully purified by the train sublimation method more than twice.[24] Single crystals of both materials were grown from the vapor phase by sublimation. A more detailed explanation of the method of single-crystal growth is described in another report.[8h] About 100 mg of BFTT and BPTT was used for the single-crystal growth, and the outer tube was heated at 330−350 °C or 310−330 °C, respectively, under a reduced pressure of nitrogen using the same apparatus as described in the reference. The colors of the BFTT and BPTT crystals are yellow and pale yellow, and the crystal sizes of BFTT and BPTT were $0.48 \times 0.48 \times 0.01$ and $0.40 \times 0.40 \times 0.01$ (mm), respectively. A fairly good single crystal was selected by the polarized microscope (Olympus BX51) for use in the X-ray structure analysis. Data were collected at the temperature indicated in Table 1 with a Bruker Smart APEX-CCD diffractometer with Mo Kα radiation (50 kV, 90 mA) monochromated by graphite. Data reduction and an empirical absorption correction were applied by SADABS (version 6.22, Bruker AXS, Madison, WI) and SADABS (G. M. Sheldrick, University of Gottingen, Germany, 1996). The structure determination was done by using the SHELX-TL crystallographic software package (version 6.12, Bruker AXS, Madison, WI, 1997) with direct methods and refinements with a full-matrix least-squares method on F^2. All the non-hydrogen atoms were refined anisotropically. The graphics were performed using PLATON.[25]

General Methods. Organic films were observed by the AFM in the tapping mode. The AFM system used in this study was a NanoScope III (Digital Instruments, Inc., Santa Barbara, CA). The measurements were performed in air at room temperature, and all images were obtained in the tapping mode. A cantilever with a spring constant of 0.12 N/m was used at a scanning rate of 2−3 Hz. XRD measurements of the evaporated films on silicon oxide coated silicon wafers were performed in $\theta-2\theta$ continuous scans using a RU-300 powder diffractometer (Rigaku Co., Tokyo) with Cu Kα radiation. UPS was measured by means of an AC-2 machine. (Riken Keike. Co., Ltd., Tokyo) CV was performed using an Autolab PGSTAT30 pontentiostat/galvanostat with a three-electrode cell in a solution of 0.1 M tetrabutylammonium perchlorate dissolved in acetonitrile at a scan rate of 50 mV/s. The thin films of oligomers were deposited on an ITO electrode by thermal evaporation in a high vacuum (2×10^{-6} Torr). A Pt wire and Ag/$AgNO_3$ (0.1 M) electrode were used as the counter and the reference electrodes, respectively. Its potential was corrected to the saturated calomel electrode (SCE; 0.31 V vs SCE) by measuring the ferrocene/ferrocenium couple in this system. HOMO energies were estimated using the following equation:[26] $\text{HOMO} = 4.44 + E_{\text{oxa}}^{\text{onset}}$. The band gaps were measured according to the onset absorption of a UV−vis spectroscope.

Device Fabrication. A thin film organic semiconducting layer (about 50 nm measured by a quartz-crystal thickness monitor) was deposited on a SiO_2 (300 nm, 10 nF/cm^2) surface on a heavily doped silicon wafer, as the gate electrode, at a deposition rate of 0.01−0.04 nm/s. The SiO_2 surfaces were pretreated with HMDS and kept at various substrate temperatures during the deposition. After evaporation, the OFETs were completed by evaporating gold through a shadow mask to form source and drain electrodes on the semiconducting thin films as a top contact geometry. This device has a channel length and width of 20 μm and 5 mm, respectively. The OFETs characteristics were measured with a KEITHLEY 4200 semiconductor characterization system in an air atmosphere. The UV stability of the devices with respect to photooxidation was determined after UV irradiation at a wavelength of 380 nm using a Hamamatsu LC5 instrument (50 mW/cm^2). FT-IR transmission spectra were measured using a Perkin Elmer system 2000 FT-IR.

Acknowledgment. This work was financially supported by the Korea Science and Engineering Foundation (KOSEF) via the National Research Laboratory (NRL) program, Ministry of Education of Korea through BK21 program (GIST), Program for Integrated Molecular System (GIST), Center for Advanced Functional Polymers (CAFPoly) through KOSEF (KAIST), and the Information Display R&D Center (No. AOD-02-A) through 21st Century Frontier R&D Program of Ministry of Science and Technology (MOST). One of the authors (Y.-Y.N.) was supported by KOSEF during a visit to AIST.

Note Added after ASAP Publication. There were errors in the description of the bending angles of BPTT and in the description of the software and equipment used in the single-crystal structure analysis in the version published ASAP June 18, 2005; the corrected version was published ASAP June 22, 2005.

Supporting Information Available: X-ray crystallographic files (CIF), calculated shortest intermolecular distances, and absorption and PL spectra for BFTT and BPTT. This material is available free of charge via the Internet at http://pubs.acs.org.

CM0504889

(22) Lim, E.; Jung, B. J.; Shim, H. K. *Macromolecules* **2003**, *36*, 4288.
(23) Hotta, S.; Kimura, H.; Lee, S. A.; Tamaki, T. *J. Heterocycl. Chem.* **2000**, *37*, 281.
(24) Forrest, S. R. *Chem. Rev.* **1997**, *97*, 1793.
(25) Spek, A. L. *Acta Crystallogr., Sect. A.* **1990**, *46*, C34.
(26) (a) de Leeuw, D. M.; Simenon, M. M. J.; Brown, A. R.; Einerhand, R. E. F. *Synth. Met.* **1997**, *87*, 53. (b) Nessakh, B.; Horowitz, G.; Garnier, F.; Deloffre, F.; Srivastava, P.; Yassar, A. *J. Electroanal. Chem.* **1995**, *399*, 97.